

Admissible Control Laws for Constrained Linear Power Flow: The General Case

Edwin Mora and Florian Steinke

Abstract—Linearized power flow with line flow and voltage constraints can be modeled as a system of linear inequalities depending on the power injections. When some injections are controlled by the grid operator while others are determined exogenously, robust control aims at determining grid operator’s actions under imperfect system observability such that the grid state is feasible for all possible realizations of the exogenous actions. It was shown how to design and analyze such admissible control policies efficiently for the subclass of affine control laws, but this paper shows that there are important cases that require more general control policies. We show that, for the constrained linear power flow setting, general admissible control policies can always be chosen as piecewise affine (PWA) mappings. The PWA mapping can be explicitly characterized offline or control actions can be computed online by solving an optimization problem given a current observation. For the latter setup, we provide an algorithm that verifies offline that the online control scheme is admissible. This verification step is a crucial precondition to apply the online control scheme in real, safety-critical power grids. The proposed framework is demonstrated with applications to voltage regulation in active distribution grids subject to uncertain prosumers and low observability.

Index Terms—Admissible control law, imperfect observability, multiparametric programming, robust power flow, verification algorithm.

NOMENCLATURE

$j \in \mathbb{C}$	Imaginary unit $j = \sqrt{-1}$.
$r_{ij} \in \mathbb{R}_{>0}$	Resistance of the line connecting buses (i, j) .
$x_{ij} \in \mathbb{R}_{>0}$	Reactance of the line connecting buses (i, j) .
$p_i \in \mathbb{R}$	Active power injection at bus i .
$q_i \in \mathbb{R}$	Reactive power injection at bus i .
$s_i \in \mathbb{C}$	Apparent power injection at bus i .
$v_i \in \mathbb{R}_{>0}$	Voltage magnitude at bus i .
$\eta \in \mathbb{R}$	Feasibility indicator.
$\mathbf{x} \in \mathbb{R}^{n_x}$	Grid state (e.g., voltage magnitudes or angles).
$\mathbf{u} \in \mathbb{R}^{n_u}$	Control action.
$\mathbf{d} \in \mathbb{R}^{n_d}$	Exogenous action.
$\mathbf{y} \in \mathbb{R}^{n_y}$	Vector of measured quantities.
$\hat{\mathbf{y}} \in \mathbb{R}^{n_y}$	Observation (part of \mathbf{y} associated to \mathbf{d}).
$\mathcal{X} \subset \mathbb{R}^{n_x}$	Set of feasible grid states.
$\mathcal{U} \subset \mathbb{R}^{n_u}$	Set of control actions.
$\mathcal{D} \subset \mathbb{R}^{n_d}$	Set of exogenous actions.
$\hat{\mathcal{Y}} \subset \mathbb{R}^{n_y}$	Set of possible observations.
$n_z \in \mathbb{Z}_{>0}$	Number of operational constraints.
$\mathbf{1}$	Vector of ones of suitable dimension.

The authors are with the Energy Information Networks and Systems Lab at TU Darmstadt, 64183 Darmstadt, Germany (e-mail: edwin.mora@gmail.com; florian.steinke@eins.tu-darmstadt.de). This work was sponsored by the German Federal Ministry of Education and Research in project AlgoRes (grant no. 01|S18066A). It has been performed in the context of the LOEWE center emergenCITY. This paper has been accepted for publication by IEEE. DOI: 10.1109/TPWRS.2023.3263365.

I. INTRODUCTION

Today’s power grids face increasing operational challenges due to the variability and uncertainty of various power in-feeds. Next to classic load uncertainty considerations, photovoltaic (PV) fluctuations play an increasing role, often leading to undesired over- and/or undervoltages in distribution grids [1]. The charging of electric vehicles may lead to power overloads in lines and transformers [2]. Transmission grids have to react flexibly to the aggregated uncertainties arising from the distribution grids but also to centralized sources of variability such as large wind parks [3]. Since at the same time more and more sensors and actuators are available in the grids, suitable controllers can alleviate many of these challenges.

The control of power grids at steady state with uncertain in-feeds can be based on stochastic [4]–[6] or robust [3], [7], [8] principles. Robustness means that for any realization of the uncertain factors, the system remains in a feasible state. This criterion has been used in [8] to efficiently compute affine control laws for linearized power flow problems with line flow or voltage constraints and static, time-constant uncertainties. However, the simulation experiments presented in this paper show that, within this setup, there are relevant situations where an admissible affine control law does not exist, but a more general admissible control law does. This motivates the following research questions addressed in this paper: What are the properties of such more general admissible control laws? How can we prove their existence and compute them efficiently?

Previous work investigated a two-stage optimization algorithm [9] that uses a given system observation to determine on-the-fly a control action guaranteeing the feasibility of the grid state independently of the uncertain power in-feeds, if possible. The present paper complements this work with several novel contributions related to real-time optimal power flow approaches [10]. First, we show how to explicitly characterize the complete control law offline using multiparametric linear programming techniques [11]–[13]. This is the key to prove that for the constrained linear power flow setting general admissible control laws can always be chosen as PWA mappings, where each affine piece is defined on a convex polytopic set. This is a non-trivial derivation from multiparametric linear programming theory since, unlike common applications where the right-hand side or the objective of the associated linear program (LP) are varied, in our case the system matrix is varying parametrically. Given this novel characterization, one can store the PWA control law in a parametric form similarly to explicit model predictive control approaches [14], [15].

Since the explicit form may have exponentially many pieces,

it may often be more efficient to stay with online computations or to combine explicit and online computations [16]. However, in this case, it is important to know prior to the controller implementation whether the online computations will always result in control actions that lead to feasible system states. A second novel contribution of this paper is an algorithm that checks this admissibility condition offline. The proposed approach is based on a non-convex Quadratically Constrained Quadratic Program (QCQP). It is derived from an equivalent one-stage formulation of the two-stage optimization algorithm obtained by applying duality theory [17]. The contribution is a key enabler to deploy the online control scheme, and thereby general PWA control laws, in practical, safety-critical infrastructures. Grid operators need to be sure about the admissibility of the controller already in the planning stage.

The theoretical results and algorithms obtained in this paper are evaluated with two examples of voltage regulation in distribution grids subject to uncertain prosumers and limited observability and controllability. First, a demonstration of all design steps is conducted for a simple 3 bus feeder. Subsequently, the proposed techniques are applied to a modified version of the IEEE 123 bus test case with high penetration of PV. In both cases, the performance of the obtained control laws is assessed within the assumed linear model as well as with non-linear Alternating Current Power Flow (ACPF) simulations.

The rest of this paper is organized as follows. Section II reviews the theory on admissible control laws for constrained static linear power flow systems from [8], [9]. Section III presents an algorithm to explicitly compute the full control law (if it exists) and provides the proof of its characterization as a PWA mapping. Section IV introduces the QCQP that verifies the admissibility of the online control scheme. Section V explains an implementation trick that reduces the computation time of the QCQP by orders of magnitude. The power system application examples are presented and discussed in Section VI, before concluding in Section VII.

II. BACKGROUND

This section reviews the modeling of constrained linear power flow at steady state as a set of linear (in)equalities. The proposed modeling technique can be applied to both transmission and distribution grids as explained in [8], [9] and is illustrated with a simple distribution feeder example. Subsequently, we review the definition of admissible control laws for such systems as introduced in [8].

A. Power Flow as a Constrained Static Linear System

Consider an abstract, linear, steady state power flow representation of the form

$$\mathbf{x} = \mathbf{B}\mathbf{u} + \mathbf{F}\mathbf{d}, \quad (1)$$

where $\mathbf{x} \in \mathbb{R}^{n_x}$ is the *state* of the power grid, which is defined by, for example, the nodal voltage magnitudes.¹ The state is

¹Depending on the application, the state \mathbf{x} can be defined in terms of the voltage magnitudes, the voltage phase angles, or a combination of both. The proposed abstract representation also admits a state definition in terms of the real and imaginary part of the voltages. Please refer to [18] for a recent review on power flow modeling.

determined by the *control action* $\mathbf{u} \in \mathbb{R}^{n_u}$ and the *exogenous action* $\mathbf{d} \in \mathbb{R}^{n_d}$. The control action \mathbf{u} models quantities that the grid operator can manipulate. They comprise, for instance, the nodal active or reactive power to be injected by controlled generation units or the tap position of transformers.² The exogenous action \mathbf{d} represents the power injections being determined by other system users, e.g., the power demand or the active power generated by decentralized, non-controlled generation units. The matrices $\mathbf{B} \in \mathbb{R}^{n_x \times n_u}$ and $\mathbf{F} \in \mathbb{R}^{n_x \times n_d}$ are assumed to be known to the grid operator. They can be derived from the physical grid parameters as discussed below.

In power grid operations, the grid operator periodically determines the value of the control action \mathbf{u} based on available information about the state \mathbf{x} of the grid. However, the vector quantities \mathbf{x} and \mathbf{d} are usually not directly accessible to the grid operator due to technical, economical, or privacy reasons. Instead, a typically small number of *measured quantities* $\mathbf{y} \in \mathbb{R}^{n_y}$ are available. Examples of measured quantities are line flows, nodal voltage magnitudes, or nodal power in-feeds. We assume that the measured quantities \mathbf{y} are also determined linearly by the state \mathbf{x} which, under consideration of (1), can be expressed in terms of the actions (\mathbf{u}, \mathbf{d}) in the form

$$\mathbf{y} = \mathbf{N}\mathbf{u} + \mathbf{M}\mathbf{d}, \quad (2)$$

where the matrices $\mathbf{N} \in \mathbb{R}^{n_y \times n_u}$ and $\mathbf{M} \in \mathbb{R}^{n_y \times n_d}$ are assumed to be known to the grid operator.

In practical applications, the quantities $(\mathbf{x}, \mathbf{u}, \mathbf{d})$ have to fulfill a set of engineering requirements. Depending on the application, there are pre-specified ranges of admissible values for the nodal voltage magnitudes as well as for the power capacity of the transmission lines and transformers. The power produced/consumed by both controlled and uncontrolled prosumers in the grid is also subject to technical limitations.

We thus define $\mathbf{u} \in \mathcal{U} \subset \mathbb{R}^{n_u}$ and $\mathbf{d} \in \mathcal{D} \subset \mathbb{R}^{n_d}$, where the *set of control actions* \mathcal{U} and the *uncertainty set* \mathcal{D} are assumed to be convex polytopes, i.e.,

$$\mathcal{U} = \{\mathbf{u} \in \mathbb{R}^{n_u}: \mathbf{R}\mathbf{u} \leq \mathbf{r}\}, \quad \mathcal{D} = \{\mathbf{d} \in \mathbb{R}^{n_d}: \mathbf{T}\mathbf{d} \leq \mathbf{t}\}. \quad (3)$$

The parameters $\mathbf{R} \in \mathbb{R}^{l_u \times n_u}$, $\mathbf{r} \in \mathbb{R}^{l_u}$, $\mathbf{T} \in \mathbb{R}^{l_d \times n_d}$, and $\mathbf{t} \in \mathbb{R}^{l_d}$ are supposed to be known a priori. In addition, we say that the state \mathbf{x} is *feasible* if it is in *feasibility set* $\mathcal{X} \in \mathbb{R}^{n_x}$. The feasibility set \mathcal{X} is assumed to be defined by a set of linear inequalities of the form $\mathbf{E}\mathbf{x} \leq \mathbf{b}$, with a priori known parameters $\mathbf{E} \in \mathbb{R}^{n_z \times n_x}$ and $\mathbf{b} \in \mathbb{R}^{n_z}$. Due to the linear relation (1) between the state \mathbf{x} and the actions (\mathbf{u}, \mathbf{d}) , the state is feasible if the actions fulfill

$$\mathbf{G}\mathbf{u} + \mathbf{H}\mathbf{d} \leq \mathbf{b}, \quad (4)$$

where $\mathbf{G} = \mathbf{E}\mathbf{B}$ and $\mathbf{H} = \mathbf{E}\mathbf{F}$.

A constrained linear, steady state power flow system is then fully described by the linear (in)equalities (2)–(4). This modeling framework was applied to solve power flow control problems in both transmission [8] and distribution grids [9]. In the following, we illustrate how to apply it to an exemplary distribution feeder.

²Note that the control action \mathbf{u} is defined here in a continuous space. The simulation experiments discussed in Section VI illustrate how to adapt the proposed control strategies to discrete control actions.

Example 1. Consider the power distribution feeder shown in Fig. 1. The feeder has two prosumers, the first connected to bus 1 and the second to bus 2. The substation transformer located at bus 0 is connected to bus 1 through a transmission line. This transmission line is modeled as a series impedance with resistance $r_{01} \in \mathbb{R}_{>0}$ and reactance $x_{01} \in \mathbb{R}_{>0}$. Another transmission line with electrical parameters $r_{12} \in \mathbb{R}_{>0}$ and $x_{12} \in \mathbb{R}_{>0}$ connects buses 1 and 2. The goal of the grid operator is to keep all voltage magnitudes always within the limits $\underline{v} \in \mathbb{R}_{>0}$ and $\bar{v} \in \mathbb{R}_{>0}$.

The distribution feeder can be modeled by using a lossless, linearized version of the *DistFlow* equations [19], [20].³ The voltage magnitudes $v_1, v_2 \in \mathbb{R}$ are then influenced linearly by the voltage at the root node v_0 as well as by the active and reactive power injections $p_1, p_2 \in \mathbb{R}$ and $q_1, q_2 \in \mathbb{R}$. Using the active sign convention for power, the resulting system of linear (in)equalities for the voltage magnitudes is given by

$$\begin{bmatrix} \underline{v} \\ \underline{v} \end{bmatrix} \leq \begin{bmatrix} v_1 \\ v_2 \end{bmatrix} \leq \begin{bmatrix} \bar{v} \\ \bar{v} \end{bmatrix} \Rightarrow \underbrace{\begin{bmatrix} \mathbf{I} \\ -\mathbf{I} \end{bmatrix}}_{\mathbf{E}} \underbrace{\begin{bmatrix} v_1 \\ v_2 \end{bmatrix}}_{\mathbf{x}} \leq \underbrace{\begin{bmatrix} \bar{v}\mathbf{1} \\ -\underline{v}\mathbf{1} \end{bmatrix}}_{\mathbf{b}}$$

and

$$\underbrace{\begin{bmatrix} v_1 \\ v_2 \end{bmatrix}}_{\mathbf{x}} = \underbrace{\begin{bmatrix} 1 \\ 1 \end{bmatrix}}_{\mathbf{B}} \underbrace{v_0}_{\mathbf{u}} + \underbrace{\begin{bmatrix} r_{01} & 0 & x_{01} & 0 \\ r_{01} & r_{12} & x_{01} & x_{12} \end{bmatrix}}_{\mathbf{F}} \underbrace{\begin{bmatrix} p_1 \\ p_2 \\ q_1 \\ q_2 \end{bmatrix}}_{\mathbf{d}},$$

where the identity matrix \mathbf{I} and the vector of ones $\mathbf{1}$ have appropriate dimensions. Further, the measured quantities given in Fig. 1 comprise the active and reactive power at the substation transformer (p_0, q_0) , which yields

$$\underbrace{\begin{bmatrix} p_0 \\ q_0 \end{bmatrix}}_{\mathbf{y}} = \underbrace{\begin{bmatrix} 0 \\ 0 \end{bmatrix}}_{\mathbf{N}} \underbrace{v_0}_{\mathbf{u}} + \underbrace{\begin{bmatrix} -1 & -1 & 0 & 0 \\ 0 & 0 & -1 & -1 \end{bmatrix}}_{\mathbf{M}} \underbrace{\begin{bmatrix} p_1 \\ p_2 \\ q_1 \\ q_2 \end{bmatrix}}_{\mathbf{d}}.$$

As illustrated in Fig. 1, the grid operator can manipulate the voltage magnitude v_2 based on the power at the substation transformer. The power injections at buses 1 and 2 thus represent exogenous actions being uncertain to the controller. Note that the control action space \mathcal{U} is defined by the interval of admissible voltages at bus 0, i.e., $\mathcal{U} = [\underline{v}, \bar{v}]$. The uncertainty set \mathcal{D} is given by the Cartesian product of intervals

$$\mathcal{D} = [\underline{p}_1, \bar{p}_1] \times [\underline{p}_2, \bar{p}_2] \times [\underline{q}_1, \bar{q}_1] \times [\underline{q}_2, \bar{q}_2].$$

The parameters $(\mathbf{R}, \mathbf{r}, \mathbf{T}, \mathbf{t})$ can readily be obtained from the above definitions of \mathcal{U} and \mathcal{D} . \square

For the grid of Example 1, the grid operator has to ensure the feasibility of the state for all possible realizations of the uncertain power injections $\mathbf{d} \in \mathcal{D}$. To this end, the operator has to find, if possible, an *admissible control law* $\mathbf{u} = \mathbf{k}(\mathbf{y})$, with $\mathbf{u} = v_0$ and $\mathbf{y} = [p_0 \ q_0]^\top$. The concept of admissible control law was introduced in [8] and is reviewed next.

³The choice of the lossless, linearized Distflow model is not necessary. It has only the aim of illustrating how to apply the control strategies proposed in this paper to voltage regulation in active distribution grids.

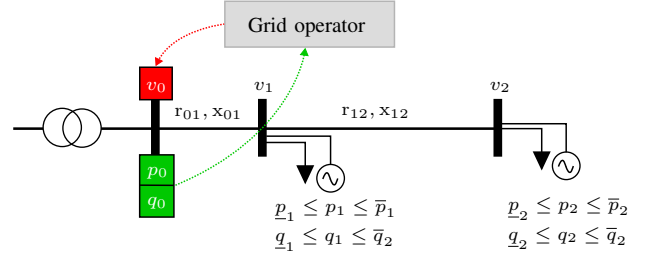


Fig. 1. Single line diagram of a simple distribution feeder with voltage control. The grid operator periodically manipulates the voltage level v_0 (the red box) based on measurements of the power (p_0, q_0) at the substation transformer (the boxes filled in green). The power at buses 1 and 2 is not determined by the grid operator, but by independent electricity prosumers. The grid operator can, however, assume bounds on these uncertain prosumers.

B. Admissible Control Laws

As indicated above, the grid operator makes periodic decisions on how to suitably adapt the value of the control action \mathbf{u} based on the measured quantities \mathbf{y} by implementing a control law $\mathbf{u} = \mathbf{k}(\mathbf{y})$. Here it is important to note that, in the steady state setting, the control law $\mathbf{u} = \mathbf{k}(\mathbf{y})$ defines a recursive mapping as the value of \mathbf{y} also depends on the choice of \mathbf{u} according to (2). However, the control law can also be expressed in terms of the part $\hat{\mathbf{y}}$ of \mathbf{y} related to the exogenous action \mathbf{d} only, since the control action \mathbf{u} is known to the grid operator and its influence on \mathbf{y} can be subtracted, i.e., $\hat{\mathbf{y}} = \mathbf{y} - \mathbf{N}\mathbf{u}$. This approach is shown in Fig. 2. We can thus equivalently consider the alternative control law $\mathbf{u} = \hat{\mathbf{k}}(\hat{\mathbf{y}})$, where $\hat{\mathbf{y}} = \mathbf{M}\mathbf{d}$ is from now on called the *observation*.

The control law $\mathbf{u} = \hat{\mathbf{k}}(\hat{\mathbf{y}})$ has to be designed such that it guarantees a feasible grid state independently of the value of the exogenous action $\mathbf{d} \in \mathcal{D}$. If the control law $\mathbf{u} = \hat{\mathbf{k}}(\hat{\mathbf{y}})$ satisfies such condition, then we say that it is *admissible*. This idea is formalized as follows.

Definition 1. The control law $\hat{\mathbf{k}} : \hat{\mathcal{Y}} \rightarrow \mathcal{U}$ is admissible if

$$\forall \mathbf{d} \in \mathcal{D} : \mathbf{G}\hat{\mathbf{k}}(\hat{\mathbf{y}}) + \mathbf{H}\mathbf{d} \leq \mathbf{b}, \quad (5)$$

with $\hat{\mathbf{y}} = \mathbf{M}\mathbf{d}$ and $\hat{\mathcal{Y}} = \mathbf{M}(\mathcal{D})$.

Note in Definition 1 that the admissibility property of the control law $\mathbf{u} = \hat{\mathbf{k}}(\hat{\mathbf{y}})$ is defined for the constrained linear power flow setting assumed in this paper. A formal analysis on the admissibility of control laws for the constrained non-linear ACPF setting is beyond the scope of this paper.

Definition 1 is exploited in subsequent sections to derive algorithms for verifying the existence of admissible control laws for a given constrained linear power system (2)–(4) and, if possible, computing an admissible controller realization.

III. COMPUTING ADMISSIBLE CONTROL LAWS

The control law computation task consists of finding the mapping $\mathbf{u} = \hat{\mathbf{k}}(\hat{\mathbf{y}})$ that assigns a control action $\mathbf{u} \in \mathcal{U}$ to each observation $\hat{\mathbf{y}} \in \hat{\mathcal{Y}}$ such that condition (5) is fulfilled. Depending on the application, the control law $\mathbf{u} = \hat{\mathbf{k}}(\hat{\mathbf{y}})$ can be expressed in several manners. For instance, the control law can be provided either in explicit, analytical form, or as a mathematical optimization problem to be solved on-the-fly

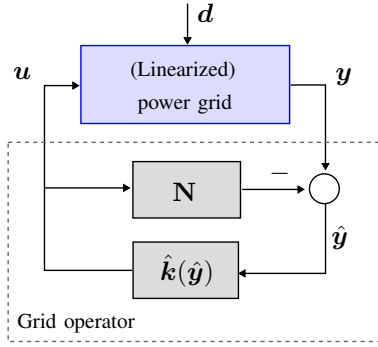


Fig. 2. The control scheme used in this paper. Given a linear representation of the power flow (2)–(4), the grid operator chooses the control action $\mathbf{u} \in \mathcal{U}$ based on the part of the measured output \mathbf{y} that captures the influence of the exogenous action $\mathbf{d} \in \mathcal{D}$, i.e., $\hat{\mathbf{y}} = \mathbf{y} - \mathbf{N}\mathbf{u} = \mathbf{M}\mathbf{d}$.

whenever a new observation is available. The former approach is called *offline* computation of the control law in this paper, the latter *online*.

A simple example for an offline computable control law is the affine mapping $\mathbf{u} = \hat{\mathbf{K}}\hat{\mathbf{y}} + \hat{\mathbf{w}}$, where the controller parameters $\hat{\mathbf{K}} \in \mathbb{R}^{n_u \times n_y}$ and $\hat{\mathbf{w}} \in \mathbb{R}^{n_u}$ are to be designed such that the admissibility condition (5) is fulfilled. In previous work [8] we show that, if an admissible affine control law exists, then the controller parameters $(\hat{\mathbf{K}}, \hat{\mathbf{w}})$ can efficiently be found by solving a LP. However, the affine linearity assumption is overly restrictive, i.e., there exist relevant cases where no admissible affine control law exists, but a more general control law does. This is illustrated with the use cases presented in Section VI. The following section introduces online and offline approaches for computing general admissible control laws, if they exist.

A. Online Two-stage Approach

The control action \mathbf{u} can be computed online for a given observation $\hat{\mathbf{y}} \in \hat{\mathcal{Y}}$ through the two-stage optimization algorithm described next.

1) *Observation-dependent Worst-case Characterization:* For any given observation $\hat{\mathbf{y}} \in \hat{\mathcal{Y}}$, the algorithm first seeks the exogenous actions in the set \mathcal{D} that maximize the impact on each constraint of the system (5) and that are consistent with the observation.

For each $j = 1, \dots, n_z$, let $\mathbf{H}^j \in \mathbb{R}^{1 \times n_d}$ represent the j th row of \mathbf{H} and $\hat{z}_j : \hat{\mathcal{Y}} \rightarrow \mathbb{R}$ be the mapping that outputs the maximum possible value of $\mathbf{H}^j \mathbf{d}$ that is consistent with observation $\hat{\mathbf{y}}$. The mapping $\hat{z}_j(\hat{\mathbf{y}})$ is defined by the LP

$$\begin{aligned} \hat{z}_j(\hat{\mathbf{y}}) = \max_{\mathbf{d} \in \mathbb{R}^{n_d}} \mathbf{H}^j \mathbf{d} \\ \text{s.t. } \mathbf{M}\mathbf{d} = \hat{\mathbf{y}}, \\ \mathbf{T}\mathbf{d} \leq \mathbf{t}. \end{aligned} \quad (6)$$

Observe in LP (6) that the decision variable \mathbf{d} is subject to an observation-dependent uncertainty set.

2) *Control Action Computation:* By solving LP (6) for the given $\hat{\mathbf{y}}$ and for all $j = 1, \dots, n_z$, we obtain the value of the vector-valued function $\hat{\mathbf{z}}(\hat{\mathbf{y}})$ which is then used to compute the control action \mathbf{u} by solving the following LP

$$\begin{aligned} \mathbf{u} = \hat{\mathbf{k}}(\hat{\mathbf{y}}) = \arg \min_{\mathbf{u}' \in \mathbb{R}^{n_u}} \min_{\eta \in \mathbb{R}} \eta \\ \text{s.t. } \mathbf{G}\mathbf{u}' + \hat{\mathbf{z}}(\hat{\mathbf{y}}) \leq \mathbf{b} + \eta \mathbf{1}, \\ \mathbf{R}\mathbf{u}' \leq \mathbf{r}. \end{aligned} \quad (7)$$

Note in LP (7) that the decision variable η represents a feasibility indicator for the resulting \mathbf{u} . In other words, if for a given observation $\hat{\mathbf{y}}$ the corresponding optimal value of η is at most zero, then the associated control action \mathbf{u} guarantees a feasible system state. In the following, we use the notation $\eta^*(\hat{\mathbf{y}})$ when referring to the optimal value of η associated to $\hat{\mathbf{y}}$. The control law implied by LPs (6)–(7) is hence admissible if the condition $\eta^*(\hat{\mathbf{y}}) \leq 0$ is fulfilled for all possible $\hat{\mathbf{y}} \in \hat{\mathcal{Y}}$.

If approximate solution methods for the LPs are used, the total error of the two-stage approach can be controlled as follows. Suppose LP (6) is solved to accuracy ϵ_1 , then $\hat{z}_j(\hat{\mathbf{y}})$ is known up to this accuracy. $\hat{z}_j(\hat{\mathbf{y}})$ enters LP (7) in the first constraint block, thus, the computed η might then be wrong by up to ϵ_1 . If LP (7) is solved to accuracy ϵ_2 , then the total error of the resulting η is bounded by $\epsilon_1 + \epsilon_2$.

Choosing η as the objective function of LP (7) simplifies in Section IV the derivation of an algorithm for verifying the admissibility of the control law implied by LPs (6)–(7). However, if the existence of an admissible control law is guaranteed, the objective function of LP (7) can be chosen differently depending on the application, e.g., by removing the decision variable η and then introducing a linear or convex quadratic cost function of \mathbf{u} . This is illustrated in Section VI.

B. Online One-stage Approach

Computing the control action through the two-stage approach (6)–(7) is computationally efficient [9]. Nevertheless, it is useful to transform it into an one-stage LP for two reasons. The one-stage LP helps us prove that an admissible control law $\mathbf{u} = \hat{\mathbf{k}}(\hat{\mathbf{y}})$ can always be chosen as a PWA mapping. It is also the key to obtain in Section IV an algorithm that verifies the admissibility of the control law implied by LPs (6)–(7).

The one-stage LP formulation is obtained as follows. First, observe that the two-stage formulation (6)–(7) can be equivalently expressed as

$$\begin{aligned} \mathbf{u} = \hat{\mathbf{k}}(\hat{\mathbf{y}}) = \arg \min_{\mathbf{u}' \in \mathcal{U}} \min_{\eta \in \mathbb{R}} \eta \\ \text{s.t. } \mathbf{G}\mathbf{u}' + \underbrace{\begin{bmatrix} \max_{\mathbf{d} \in \mathcal{D}} \mathbf{H}^1 \mathbf{d} \text{ s.t. } \mathbf{M}\mathbf{d} = \hat{\mathbf{y}} \\ \vdots \\ \max_{\mathbf{d} \in \mathcal{D}} \mathbf{H}^{n_z} \mathbf{d} \text{ s.t. } \mathbf{M}\mathbf{d} = \hat{\mathbf{y}} \end{bmatrix}}_{\hat{\mathbf{z}}(\hat{\mathbf{y}})} \leq \mathbf{b} + \eta \mathbf{1}. \end{aligned} \quad (8)$$

Since the j th entry of $\hat{\mathbf{z}}(\hat{\mathbf{y}})$ with $j = 1, \dots, n_z$ yields the optimal cost of an always feasible linear maximization problem, strong duality [17] holds and the j th maximization problem can be replaced with its dual, namely

$$\begin{aligned} \hat{z}_j(\hat{\mathbf{y}}) = \min_{\substack{\boldsymbol{\rho}^j \in \mathbb{R}^{n_y}, \\ \boldsymbol{\lambda}^j \in \mathbb{R}_{\geq 0}^{n_d}}} \boldsymbol{\rho}^{j\top} \hat{\mathbf{y}} + \boldsymbol{\lambda}^{j\top} \mathbf{t} \\ \text{s.t. } \begin{bmatrix} \mathbf{M}^\top & \mathbf{T}^\top \end{bmatrix} \begin{bmatrix} \boldsymbol{\rho}^j \\ \boldsymbol{\lambda}^j \end{bmatrix} = \mathbf{H}^{j\top}, \end{aligned} \quad (9)$$

where $\boldsymbol{\rho}^j \in \mathbb{R}^{n_y}$ and $\boldsymbol{\lambda}^j \in \mathbb{R}_{\geq 0}^{l_d}$ symbolize the dual variables associated to the constraints $\mathbf{M}\mathbf{d} = \hat{\mathbf{y}}$ and $\mathbf{T}\mathbf{d} \leq \mathbf{t}$ of the j th LP (6), respectively. The control action \mathbf{u} associated to the observation $\hat{\mathbf{y}}$ can then be computed via the LP formulation

$$\begin{aligned} \mathbf{u} = \hat{\mathbf{k}}(\hat{\mathbf{y}}) &= \arg \min_{\mathbf{u}' \in \mathbb{R}^{n_u}} \min_{\substack{\eta \in \mathbb{R}, \\ \boldsymbol{\rho}^1, \dots, \boldsymbol{\rho}^{n_z} \in \mathbb{R}^{n_y}, \\ \boldsymbol{\lambda}^1, \dots, \boldsymbol{\lambda}^{n_z} \in \mathbb{R}_{\geq 0}^{l_d}}} \eta \\ \text{s.t. } \mathbf{G}\mathbf{u}' + \begin{bmatrix} \boldsymbol{\rho}^{1\top} \\ \vdots \\ \boldsymbol{\rho}^{n_z\top} \end{bmatrix} \hat{\mathbf{y}} + \begin{bmatrix} \boldsymbol{\lambda}^{1\top} \\ \vdots \\ \boldsymbol{\lambda}^{n_z\top} \end{bmatrix} \mathbf{t} - \eta \mathbf{1} &\leq \mathbf{b}, \quad (10) \\ [\mathbf{M}^\top \quad \mathbf{T}^\top] \begin{bmatrix} \boldsymbol{\rho}^1 \cdots \boldsymbol{\rho}^{n_z} \\ \boldsymbol{\lambda}^1 \cdots \boldsymbol{\lambda}^{n_z} \end{bmatrix} &= \mathbf{H}^\top, \\ \mathbf{R}\mathbf{u}' &\leq \mathbf{r}. \end{aligned}$$

Note that, when replacing the n_z instances of LP (6) with their duals in expression (8), moving the inner minimization operator over $(\boldsymbol{\rho}, \boldsymbol{\lambda})$ to the outer level leads to the equivalent formulation (10) since any optimal solution of (10) is feasible for (8)–(9) yielding the same objective value and vice versa.

Formulation (10) is a LP for a fixed observation $\hat{\mathbf{y}}$. As formulations (10) and (6)–(7) are equivalent, the control law $\mathbf{u} = \hat{\mathbf{k}}(\hat{\mathbf{y}})$ implied by LP (10) is admissible if the condition $\eta^*(\hat{\mathbf{y}}) \leq 0$ is fulfilled for all possible $\hat{\mathbf{y}} \in \hat{\mathcal{Y}}$.⁴

C. Offline Approach

Instead of solving either LP (10) or LPs (6)–(7) online, we now focus on finding an explicit, closed-form representation for the control law $\mathbf{u} = \hat{\mathbf{k}}(\hat{\mathbf{y}})$ over all $\hat{\mathbf{y}} \in \hat{\mathcal{Y}}$. This is particularly beneficial for small-sized problem instances since the computation of the control action \mathbf{u} turns into evaluating an analytic function of the observation $\hat{\mathbf{y}}$. Even more interestingly, the offline approach proposed next yields the proof that admissible control laws for the constrained linear power flow setting (2)–(4) can always be chosen as PWA mappings.

Closed-form expressions for the control law $\mathbf{u} = \hat{\mathbf{k}}(\hat{\mathbf{y}})$ can be computed by solving LP (10) for all possible observations $\hat{\mathbf{y}} \in \hat{\mathcal{Y}}$. This task corresponds to computing the explicit solution of a multiparametric linear program (MPLP) with parametric system matrix, since for each $j = 1, \dots, n_z$ the parameter $\hat{\mathbf{y}}$ appears multiplied with the optimization variable $\boldsymbol{\rho}^j$ in the first set of inequality constraints in formulation (10).

When the right-hand side or the objective of a MPLP are parametric it is known that the solution functions are PWA [21] and the associated regions in the parameter space, the so-called *critical regions*, convex polyhedra [13]. If the system matrix is parametric, as in our case, both characterizations are not necessarily fulfilled as can be deduced from [22, Theorem 4.3]. This makes computing and storing an explicit solution representation not easy in general.

However, we can show that for our special problem instance the two properties are still fulfilled. This allows us to compute and store a closed-form expression of $\mathbf{u} = \hat{\mathbf{k}}(\hat{\mathbf{y}})$ with known software tools.

⁴It is shown in Section VI that the solver time of the two-stage approach (6)–(7) often outperforms the solvet time of the one-stage approach (10).

Theorem 1. *The control law implied by LP (10) is a PWA mapping with pieces defined on convex polytopes.*

Proof. To proof Theorem 1, we return to the two-stage approach (6)–(7) for computing the control law, but now in a parametric fashion.

1) *Closed-form of the Mapping $\hat{\mathbf{z}}(\hat{\mathbf{y}})$:* The first-stage LP (6) is a MPLP with right-hand side parameter $\hat{\mathbf{y}} \in \hat{\mathcal{Y}}$. Since the set \mathcal{D} is a convex polytope, the set $\hat{\mathcal{Y}} = \mathbf{M}(\mathcal{D})$ is also a convex polytope and the following results apply.

Corollary 1 ([21]). *For any $j \in \{1, \dots, n_z\}$, the mapping $\hat{z}_j : \hat{\mathcal{Y}} \rightarrow \mathbb{R}$ defined as in (6) is piecewise affine, continuous, and concave.*

Corollary 2 ([13]). *For any $j \in \{1, \dots, n_z\}$, the critical regions of $\hat{\mathcal{Y}}$ associated to the mapping $\hat{z}_j(\hat{\mathbf{y}})$ are convex polytopes.*

Now note that instead of computing the parametric solution of each mapping $\hat{z}_j(\hat{\mathbf{y}})$ separately we can equivalently compute parametric solution of the vector-valued mapping $\hat{\mathbf{z}}(\hat{\mathbf{y}})$ by means of the single, larger formulation

$$\begin{aligned} \hat{\mathbf{z}}(\hat{\mathbf{y}}) &= \arg \max_{\hat{\mathbf{z}} \in \mathbb{R}^{n_z}} \max_{\hat{\mathbf{d}}^1, \dots, \hat{\mathbf{d}}^{n_z} \in \mathcal{D}} \mathbf{1}^\top \hat{\mathbf{z}} \\ \text{s.t. } \hat{\mathbf{z}} &= \begin{bmatrix} \mathbf{H}^1 \hat{\mathbf{d}}^1 \\ \vdots \\ \mathbf{H}^{n_z} \hat{\mathbf{d}}^{n_z} \end{bmatrix}, \quad (11) \\ \mathbf{M}\hat{\mathbf{d}}^j &= \hat{\mathbf{y}}, \quad \forall j = 1, \dots, n_z. \end{aligned}$$

By construction, the above formulation is a MPLP with right-hand side parameter $\hat{\mathbf{y}} \in \hat{\mathcal{Y}}$. The mapping $\hat{\mathbf{z}} : \hat{\mathcal{Y}} \rightarrow \mathbb{R}^{n_z}$ is thus PWA and its associated critical regions of $\hat{\mathcal{Y}}$ are convex polytopes. Now let $\mathcal{R}^\kappa(\hat{\mathcal{Y}})$ be the κ th critical region of $\hat{\mathcal{Y}}$, with $\kappa = 1, \dots, \hat{\kappa}$. Then, the κ th piece of $\hat{\mathbf{z}}(\hat{\mathbf{y}})$, here denoted by $\hat{\mathbf{z}}^\kappa(\hat{\mathbf{y}})$, can be written in affine form as

$$\hat{\mathbf{z}}^\kappa(\hat{\mathbf{y}}) = \mathbf{\Pi}^\kappa \hat{\mathbf{y}} + \boldsymbol{\pi}^\kappa, \quad \forall \hat{\mathbf{y}} \in \mathcal{R}^\kappa(\hat{\mathcal{Y}}). \quad (12)$$

The parameters $\mathbf{\Pi}^\kappa \in \mathbb{R}^{n_z \times n_y}$ and $\boldsymbol{\pi}^\kappa \in \mathbb{R}^{n_z}$ are valid for the critical region $\mathcal{R}^\kappa(\hat{\mathcal{Y}})$ and can be readily determined for each $\kappa = 1, \dots, \hat{\kappa}$ by using off-the-shelf multiparametric linear optimization software, e.g., the Multiparametric Programming Toolbox (MPT) [23]. Note that the values that $\hat{\mathbf{z}}^\kappa(\hat{\mathbf{y}})$ maps from the elements of $\mathcal{R}^\kappa(\hat{\mathcal{Y}})$ lie also in a convex polytope.

2) *Closed-form of the Mapping $\hat{\mathbf{k}}(\hat{\mathbf{y}})$:* For the κ th critical region $\mathcal{R}^\kappa(\hat{\mathcal{Y}})$ with $\kappa = 1, \dots, \hat{\kappa}$, we now construct the mapping $\hat{\mathbf{k}}^\kappa : \mathcal{R}^\kappa(\hat{\mathcal{Y}}) \rightarrow \mathcal{U}$ based on the second-stage LP (7) as well as on expression (12). We obtain

$$\begin{aligned} \hat{\mathbf{k}}^\kappa(\hat{\mathbf{y}}) &= \arg \min_{\mathbf{u}' \in \mathcal{U}} \min_{\eta \in \mathbb{R}} \eta \\ \text{s.t. } \mathbf{G}\mathbf{u}' + \underbrace{\mathbf{\Pi}^\kappa \hat{\mathbf{y}} + \boldsymbol{\pi}^\kappa}_{\hat{\mathbf{z}}^\kappa(\hat{\mathbf{y}})} &\leq \mathbf{b} + \eta \mathbf{1}. \quad (13) \end{aligned}$$

The above problem formulation can be interpreted as a MPLP with right-hand side parameter $\hat{\mathbf{y}} \in \mathcal{R}^\kappa(\hat{\mathcal{Y}})$. This means that the mapping $\hat{\mathbf{k}}^\kappa(\hat{\mathbf{y}})$ is PWA for $\hat{\mathbf{y}} \in \mathcal{R}^\kappa(\hat{\mathcal{Y}})$ and the associated critical regions of $\mathcal{R}^\kappa(\hat{\mathcal{Y}})$ are convex polytopes.

Now let $\mathcal{R}^{l\kappa}(\hat{\mathcal{Y}})$ denote the l th critical region of $\mathcal{R}^\kappa(\hat{\mathcal{Y}})$, with $l = 1, \dots, \hat{l}_\kappa$. The l th piece of $\hat{\mathbf{k}}^\kappa(\hat{\mathbf{y}})$, here denoted by $\hat{\mathbf{k}}^{l\kappa}(\hat{\mathbf{y}})$, has the affine form

$$\hat{\mathbf{k}}^{l\kappa}(\hat{\mathbf{y}}) = \mathbf{W}^{l\kappa}\hat{\mathbf{y}} + \boldsymbol{\nu}^{l\kappa}, \quad \forall \hat{\mathbf{y}} \in \mathcal{R}^{l\kappa}(\hat{\mathcal{Y}}),$$

where $\mathbf{W}^{l\kappa} \in \mathbb{R}^{n_u \times n_y}$ and $\boldsymbol{\nu}^{l\kappa} \in \mathbb{R}^{n_u}$ are fixed parameters valid for the subset $\mathcal{R}^{l\kappa}(\hat{\mathcal{Y}})$. As before, the parameters $\mathbf{W}^{l\kappa}$, $\boldsymbol{\nu}^{l\kappa}$, and the critical regions $\mathcal{R}^{l\kappa}(\hat{\mathcal{Y}})$ can be computed for each $l = 1, \dots, \hat{l}_\kappa$ by using off-the-shelf optimization software such like MPT. Note that the resulting control law $\mathbf{u} = \hat{\mathbf{k}}(\hat{\mathbf{y}})$ has a total of $D = \sum_{\kappa=1}^{\hat{\kappa}} \hat{l}_\kappa \hat{\kappa}$ affine pieces.

From the above derivations we conclude that the control law implied by LPs (6)–(7) is a PWA mapping with pieces defined on convex polytopes. As formulations (6)–(7) and (10) are equivalent, these properties also hold for the control law implied by LP (10). \square

A well-known result in multiparametric programming is that the total number of critical regions may grow exponentially with the dimension of the parameter vector [13]. We hence recommend the proposed offline computation approach only for small-scale use cases such as the example in Section VI-A. For larger applications, see the example in Section VI-B, the online computation techniques are often more efficient. In this case, however, it is not certain that the computed control actions will imply an admissible control law. This motivates the development of the following verification algorithm that proves the admissibility of an online-computed PWA control law $\mathbf{u} = \hat{\mathbf{k}}(\hat{\mathbf{y}})$ prior to its actual implementation.

IV. VERIFYING THE EXISTENCE OF ADMISSIBLE PWA CONTROL LAWS

In this section, we address the task of verifying the admissibility of the online PWA control laws introduced in Section III. This offline verification step is crucially important to apply such control laws in real, safety-critical power grids. The proposed verification algorithm is derived from the online one-stage control law implied by LP (10) as follows.

As pointed out in Section III, the control law implied by LP (10) is admissible if the condition $\eta^*(\hat{\mathbf{y}}) \leq 0$ is fulfilled for all $\hat{\mathbf{y}} \in \hat{\mathcal{Y}}$. To verify the admissibility property of the mapping $\mathbf{u} = \hat{\mathbf{k}}(\hat{\mathbf{y}})$, we propose to seek for the worst-case realization of the observation $\hat{\mathbf{y}} \in \hat{\mathcal{Y}}$ that maximizes $\eta^*(\hat{\mathbf{y}})$. Note that this can be achieved by solving the following max-min optimization problem derived directly from LP (10):

$$\eta_{\max} = \max_{\hat{\mathbf{y}} \in \hat{\mathcal{Y}}} \min_{\substack{\eta \in \mathbb{R}, \mathbf{u}' \in \mathbb{R}^{n_u}, \\ \boldsymbol{\rho}^1, \dots, \boldsymbol{\rho}^{n_z} \in \mathbb{R}^{n_y}, \\ \boldsymbol{\lambda}^1, \dots, \boldsymbol{\lambda}^{n_z} \in \mathbb{R}_{\geq 0}^{l_d}}} \eta \quad (14)$$

s.t. constraints of LP (10).

To solve the above max-min optimization problem, we propose to apply strong duality theory again to LP (10), which allows us to reformulate problem (14) as a single non-convex QCQP as we explain next.

First, note that LP (10) is always feasible for any fixed observation $\hat{\mathbf{y}} \in \hat{\mathcal{Y}}$. Then, by strong duality, the dual formulation of optimization problem (10) corresponds to an

always feasible linear maximization problem whose optimal cost equals the optimal value of the feasibility indicator η . To derive the dual maximization problem, we now introduce the dual variables $\boldsymbol{\alpha} \in \mathbb{R}_{\leq 0}^{n_z}$, $\boldsymbol{\beta}^1, \dots, \boldsymbol{\beta}^{n_z} \in \mathbb{R}^{n_d}$, and $\boldsymbol{\gamma} \in \mathbb{R}_{\leq 0}^{l_u}$, which correspond to the first, second, and third constraint blocks of (10), respectively. Thus, each primal variable in LP (10) receives a dual constraint, which yields the following set of dual (in)equality constraints:

$$\begin{aligned} (\eta) : & \quad -\mathbf{1}^\top \boldsymbol{\alpha} = 1, \\ (\mathbf{u}') : & \quad \mathbf{G}^\top \boldsymbol{\alpha} + \mathbf{R}^\top \boldsymbol{\gamma} = 0, \\ (\boldsymbol{\rho}^j) : & \quad \alpha_j \hat{\mathbf{y}} + \mathbf{M} \boldsymbol{\beta}^j = \mathbf{0}, \quad \forall j = 1, \dots, n_z, \\ (\boldsymbol{\lambda}^j) : & \quad \alpha_j \mathbf{t} + \mathbf{T} \boldsymbol{\beta}^j \leq \mathbf{0}, \quad \forall j = 1, \dots, n_z. \end{aligned} \quad (15)$$

Moreover, the dual cost to be maximized is given by

$$\text{dual cost of LP (10)} = \mathbf{b}^\top \boldsymbol{\alpha} + \sum_{j=1}^{n_z} \mathbf{H}^j \boldsymbol{\beta}^j + \mathbf{r}^\top \boldsymbol{\gamma}, \quad (16)$$

which is readily obtained from the parameters of the right-hand side of the constraints in problem (10). The optimal dual cost equals the optimal value of η . Using the dual constraints (15) and the dual cost (16), the worst-case observation $\hat{\mathbf{y}}$ that maximizes the value of η can be found by solving

$$\begin{aligned} \eta_{\max} = & \quad \max_{\substack{\boldsymbol{\alpha} \in \mathbb{R}_{\leq 0}^{n_z}, \\ \boldsymbol{\beta}^1, \dots, \boldsymbol{\beta}^{n_z} \in \mathbb{R}^{n_d}, \\ \boldsymbol{\gamma} \in \mathbb{R}_{\leq 0}^{l_u}, \hat{\mathbf{y}} \in \hat{\mathcal{Y}}} } \mathbf{b}^\top \boldsymbol{\alpha} + \sum_{j=1}^{n_z} \mathbf{H}^j \boldsymbol{\beta}^j + \mathbf{r}^\top \boldsymbol{\gamma} \\ \text{s.t.} & \quad -\mathbf{1}^\top \boldsymbol{\alpha} = 1, \\ & \quad \mathbf{G}^\top \boldsymbol{\alpha} + \mathbf{R}^\top \boldsymbol{\gamma} = 0, \\ & \quad \alpha_j \hat{\mathbf{y}} + \mathbf{M} \boldsymbol{\beta}^j = \mathbf{0}, \quad \forall j = 1, \dots, n_z, \\ & \quad \alpha_j \mathbf{t} + \mathbf{T} \boldsymbol{\beta}^j \leq \mathbf{0}, \quad \forall j = 1, \dots, n_z. \end{aligned} \quad (17)$$

Clearly, the bilinear equality constraints involving the decision variables α_j and $\hat{\mathbf{y}}$ make the feasibility set non-convex and optimization problem (17) is a non-convex QCQP. If the optimal cost of (17) fulfills $\eta_{\max} \leq 0$, then the existence of an admissible control law is guaranteed.

While the above non-convex QCQP has worst-case exponential complexity, we found that a special implementation of the above optimization model performs efficiently in practice. This is discussed in the subsequent section.

V. IMPLEMENTATION OF THE VERIFICATION ALGORITHM

We could establish experimentally that the efficiency of solving QCQP (17) can be significantly improved by exploiting the characteristics of Gurobi 9.1.1 [24], the non-convex QCQP solver of our choice. The simple, but key step consists of isolating the bilinear terms from the linear conditions by introducing new auxiliary decision variables $\boldsymbol{\psi}^1, \dots, \boldsymbol{\psi}^{n_z} \in \mathbb{R}^{n_y}$ which are restricted as

$$\boldsymbol{\psi}^j = \alpha_j \hat{\mathbf{y}}, \quad j = 1, \dots, n_z. \quad (18)$$

This allows us to partition the constraints of QCQP (17) into a block of pure linear constraints, and the set of bilinear constraints (18) which are handled systematically in Gurobi by employing McCormick envelopes [25] and a spatial branching

strategy [26]. By recalling that $\hat{\mathbf{y}} = \mathbf{M}\mathbf{d}$, the QCQP (17) is thus equivalent to

$$\begin{aligned} \eta_{\max} = & \max_{\substack{\boldsymbol{\alpha} \in \mathbb{R}_{\leq 0}^{n_z}, \boldsymbol{\gamma} \in \mathbb{R}_{\leq 0}^{l_u}, \\ \mathbf{d}, \boldsymbol{\beta}^1, \dots, \boldsymbol{\beta}^{n_z} \in \mathbb{R}^{n_d}, \\ \hat{\mathbf{y}}, \boldsymbol{\psi}^1, \dots, \boldsymbol{\psi}^{n_z} \in \mathbb{R}^{n_y}}} \mathbf{b}^\top \boldsymbol{\alpha} + \sum_{j=1}^{n_z} \mathbf{H}^j \boldsymbol{\beta}^j + \mathbf{r}^\top \boldsymbol{\gamma} \\ \text{s.t. } & -\mathbf{1}^\top \boldsymbol{\alpha} = 1, \\ & \mathbf{G}^\top \boldsymbol{\alpha} + \mathbf{R}^\top \boldsymbol{\gamma} = 0, \\ & \alpha_j \mathbf{t} + \mathbf{T} \boldsymbol{\beta}^j \leq \mathbf{0}, \quad \forall j = 1, \dots, n_z, \\ & \mathbf{T} \mathbf{d} \leq \mathbf{t}, \\ & \hat{\mathbf{y}} = \mathbf{M} \mathbf{d}, \\ & \boldsymbol{\psi}^j + \mathbf{M} \boldsymbol{\beta}^j = \mathbf{0}, \quad \forall j = 1, \dots, n_z, \\ & \boldsymbol{\psi}^j = \alpha_j \hat{\mathbf{y}}, \quad \forall j = 1, \dots, n_z. \end{aligned} \quad (19)$$

We validate experimentally that providing the explicit partitioning of the constraints to the solver reduces the solver time by 1-2 orders of magnitude, making the QCQP (19) efficient for practical use cases. We also remark that in many cases it is not necessary to solve QCQP (19) to global optimality. This is because an upper bound for the optimal cost fulfilling $\eta_{\text{up}} \leq 0$ is sufficient to prove the existence of an admissible PWA control law, and a lower bound satisfying $\eta_{\text{lb}} > 0$ is sufficient to show that an admissible control law does not exist.

Note that, once the admissibility guarantee is obtained, an admissible PWA control law can be found via, e.g., the online two-stage algorithm presented in Section III-A. Moreover, instead of minimizing the feasibility indicator η , one could also minimize different objectives like linear or convex quadratic cost functions. This allows grid operators to choose control actions that are cost-optimal or favor certain kinds of actions, like changing reactive power set points, over others, like approximated transformer switching operations. An overview of the proposed toolchain is depicted in Fig. 3.

QCQP (19) cannot only be used to verify the existence of PWA control laws, but also to obtain insights about critical power grid states. For instance, the non-zero entries of $\boldsymbol{\alpha}$ indicate which system constraints are active when η is maximum. Moreover, the optimal value of \mathbf{d} produces the worst-case observation $\hat{\mathbf{y}}$ that maximizes η . This information is useful for determining appropriate measures in grid operation and/or grid planning to alleviate potential system limitations. This is demonstrated with the following application examples.

VI. APPLICATION TO VOLTAGE REGULATION IN ACTIVE DISTRIBUTION GRIDS

This section demonstrates the theoretical results and proposed algorithms for the computation and verification of admissible PWA control laws in power system applications. In particular, this section shows how to design robust voltage/VAR control (VVC) policies that use only a few actuators and sensors, but keep the voltage magnitudes within the desired operating region independently of the non-controlled, poorly observed power injections.

Starting with a simple distribution feeder, we demonstrate a realistic situation where the VVC control problem cannot be solved by any affine control law, but an admissible PWA

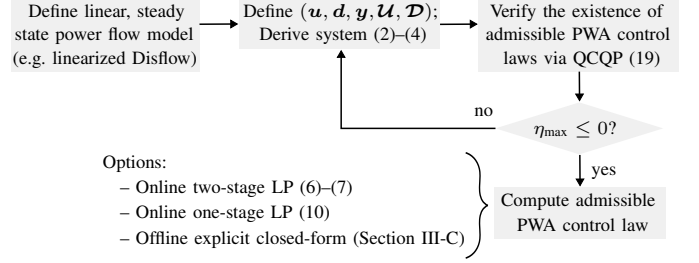


Fig. 3. Proposed toolchain for computing admissible PWA control laws for constrained linear power flow systems.

control law exists. We also study a modified version of the IEEE 123 bus test case [27] to corroborate the efficiency of the proposed algorithms to larger, realistic use cases.

In both cases, we first adopt a lossless, linearized version of the DistFlow equations [19], [20] to model the voltage magnitudes in the grid. This modeling is in line with the constrained linear system assumption of this paper and is used to compute all control laws. The performance of the obtained control laws is then evaluated empirically both within the assumed linear model and also when the non-linear AC power flow equations are used for system simulation. As no closed-form theoretical analysis is possible for ACPF, samples of the uncertain power injections are used.

The simulation experiments are implemented in Matlab 2018b, using YALMIP [28] as modeling language, Gurobi 9.1.1 as LP and QCQP solver, and MPT [23] as MPLP solver. ACPF simulations are performed using a standard Newton-Raphson approach [29] implemented in Matpower [30]. The simulations are conducted on an i5-10210U notebook with a base frequency of 1.6 GHz, and 8 GB of RAM. If not mentioned otherwise, the optimization problems are solved to an accuracy of 1×10^{-6} .

A. Simple Distribution Feeder

Fig. 4 shows the single-line diagram of a simple distribution feeder with a substation transformer and two PQ buses. Each transmission line is parametrized by a series impedance of $0.027 + j0.03$ pu. The voltage magnitude at the secondary side of the substation transformer is fixed at $v_0 = 1.01$ pu. Further, a pure active load as well as a small PV unit are connected to bus 1. This PV unit produces power with a power factor of one, i.e., $q_1 = 0$ pu. Another PV unit is connected to bus 2 and has a maximum apparent power capacity of $s_2^{\max} = 1$ pu.

The goal of the grid operator is to find an admissible control law that keeps the voltage magnitudes v_1 and v_2 within the interval $[0.95, 1.05]$ pu independently of the generation/load situation. To this end, the grid operator measures the voltage magnitude v_2 to adjust the reactive power q_2 , see Fig. 4.

The reactive power q_2 has to be chosen such that the maximum apparent power capacity of the PV unit is not exceeded. In other words, for a fixed value of generated active power p_2 , the condition $\sqrt{p_2^2 + q_2^2} \leq s_2^{\max}$ must hold. This non-linear constraint can be approximated with the help of 4 linear inequalities as shown in Fig. 4. Additionally, the maximum active power p_2 is limited to 90% of the maximum

apparent power capacity s_2^{\max} in order to still be able to support voltage regulation during peak load situations.

1) *Derivation of the Constrained Linear System:* In order to design an admissible control law with the framework proposed in this paper, we first define the quantities

$$\mathbf{u} = q_2, \quad \mathbf{y} = v_2, \quad \mathbf{d} = [p_1 \ p_2]^T.$$

As in Example 1, we adopt a linearized version DistFlow equations that neglects the line losses to derive the parameter values of the constrained static linear system (2)–(4). The voltage magnitude v_2 can then be expressed as

$$v_2 = v_0 + \underbrace{0.06}_{\mathbf{N}} \mathbf{u} + \underbrace{[0.027 \ 0.054]}_{\mathbf{M}} \mathbf{d}.$$

Moreover, the linearized operational constraints of the power grid can be expressed as

$$\underbrace{\begin{bmatrix} 0.030 \\ 0.060 \\ -0.030 \\ -0.060 \\ 0.383 \\ 0.924 \\ -0.383 \\ -0.924 \end{bmatrix}}_{\mathbf{G}} \mathbf{u} + \underbrace{\begin{bmatrix} 0.027 & 0.027 \\ 0.027 & 0.054 \\ -0.027 & -0.027 \\ -0.027 & -0.054 \\ 0 & 0.924 \\ 0 & 0.383 \\ 0 & 0.924 \\ 0 & 0.383 \end{bmatrix}}_{\mathbf{H}} \mathbf{d} \leq \underbrace{\begin{bmatrix} 0.040 \\ 0.040 \\ 0.060 \\ 0.060 \\ 0.924 \\ 0.924 \\ 0.924 \\ 0.924 \end{bmatrix}}_{\mathbf{b}},$$

where the first four inequalities are related to the operational limits for the voltage magnitudes v_1 and v_2 , and the last four inequalities correspond to the linear approximation of the operational constraint $\sqrt{p_2^2 + q_2^2} \leq s_2^{\max}$.

Following the control scheme depicted in Fig. 2, we are interested in finding an admissible control law $\hat{\mathbf{k}} : \mathcal{U} \rightarrow \hat{\mathcal{Y}}$ that uses the observation $\hat{\mathbf{y}} = \mathbf{M}\mathbf{d}$ associated to the voltage magnitude v_2 . Note that the sets \mathcal{U} , \mathcal{D} , and $\hat{\mathcal{Y}}$ can directly be obtained from the system specifications shown in Fig. 4, i.e.,

$$\begin{aligned} \mathcal{U} &= [-1, 1] \text{ pu}, \\ \mathcal{D} &= [-2.87, 0.17] \text{ pu} \times [0, 0.9] \text{ pu}, \\ \hat{\mathcal{Y}} &= [-0.078, 0.053] \text{ pu}. \end{aligned}$$

From the above set representations, the numerical values of the parameters $(\mathbf{R}, \mathbf{r}, \mathbf{T}, \mathbf{t})$ are readily derived. In the following, the existence of admissible control laws for the constrained distribution feeder is studied.

2) *Affine Control Law:* The existence of an admissible affine control law $\mathbf{u} = \hat{\mathbf{K}}\hat{\mathbf{y}} + \hat{\mathbf{w}}$, with parameters $\hat{\mathbf{K}}, \hat{\mathbf{w}} \in \mathbb{R}$, can be verified efficiently by solving the LP proposed in [8]. The best affine control law reads

$$\mathbf{u} = -5.9734\hat{\mathbf{y}} + 0.0726 \quad (20)$$

and is depicted in Fig. 5. However, the optimal solution of the LP yields $\eta_{\max} = 0.014 > 0$, meaning that the distribution grid does not admit any affine control law with the available actuators and sensors. Voltage constraint violations are thus to be expected when applying the affine control law (20) to the linearized distribution grid, see Fig. 5. The solution of the LP proposed in [8] is obtained in 2.4 ms.

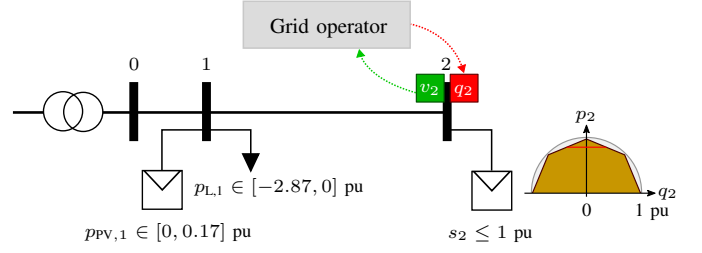


Fig. 4. A simple active distribution feeder subject to uncertain consumption and PV generation. The operational limits for the load and the PV unit connected to bus 1 are given as intervals. The red and green boxes represent the control action and measured quantity, respectively. The non-linear operational constraint for the PV unit at bus 2 is approximated with 4 linear inequalities, and the red line indicates the maximum allowed active power output p_2 that ensures sufficient reactive power capabilities during peak output.

3) *PWA Control Law:* We now verify the existence of an admissible PWA control law by solving QCQP (19). The optimal solution of the QCQP yields $\eta_{\max} = -0.0011 \leq 0$, i.e., the existence of an admissible PWA control law $\mathbf{u} = \hat{\mathbf{k}}(\hat{\mathbf{y}})$ is guaranteed. With the software and hardware specified in above, the value of η_{\max} is obtained in 11.4 ms. This admissibility guarantee ensures that the voltage magnitudes are always feasible when applying online computed control actions via LPs (6)–(7) to the linearized distribution grid. In contrast, no such theoretical guarantee is available for the corresponding non-linear ACPF system.

The admissibility guarantee is now exploited to design an admissible PWA control law that maximizes the reactive power q_2 instead of minimizing the feasibility indicator η . This objective is chosen in order to keep the voltage magnitudes as high as possible and consequently to reduce the line losses. The proposed PWA control law is thus defined by the two-stage linear optimization problem

$$\begin{aligned} \mathbf{u} = \hat{\mathbf{k}}_{\text{opt}}(\hat{\mathbf{y}}) &= \arg \max_{\mathbf{u}' \in \mathbb{R}} \mathbf{u}' \\ \text{s.t. } \mathbf{G}\mathbf{u}' + \hat{\mathbf{z}}(\hat{\mathbf{y}}) &\leq \mathbf{b}, \\ \mathbf{R}\mathbf{u}' &\leq \mathbf{r}, \end{aligned} \quad (21)$$

where $\hat{\mathbf{z}}(\hat{\mathbf{y}})$ is defined by LP (6). Note that an equivalent one-stage LP formulation for the control law $\mathbf{u} = \hat{\mathbf{k}}_{\text{opt}}(\hat{\mathbf{y}})$ is also derivable from LP (10) here.

Now the two-stage multiparametric linear optimization technique proposed in Section III-C is applied to compute the explicit closed-form expression of the PWA control law implied by LPs (6)–(21). The resulting closed-form expression has a total of 4 pieces, namely

$$\mathbf{u} = \begin{cases} -7.671\hat{\mathbf{y}} + 0.406, & \hat{\mathbf{y}} \in [-0.078, -0.039] \\ -44.708\hat{\mathbf{y}} - 1.05, & \hat{\mathbf{y}} \in [-0.039, -0.029] \\ 0.241, & \hat{\mathbf{y}} \in [-0.029, 0.026] \\ -16.667\hat{\mathbf{y}} + 0.667, & \hat{\mathbf{y}} \in [0.026, 0.053] \end{cases} \quad (22)$$

With the above software and hardware specifications, the explicit representation (22) is obtained in ca. 43 ms. Since the explicit closed-form expression of the proposed PWA control law is now available, the process of choosing the reactive power q_2 based on the voltage magnitude v_2 can be simplified

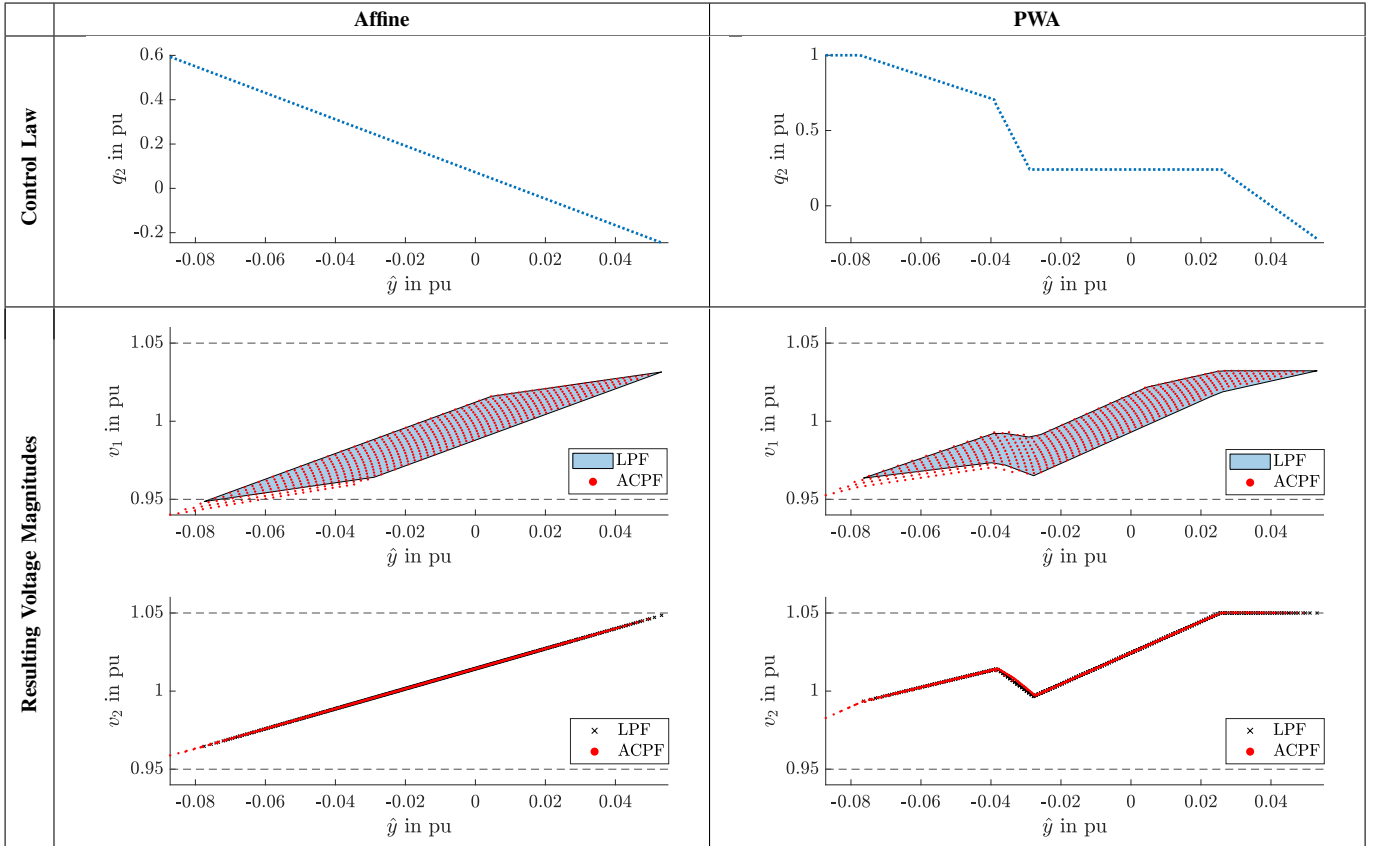


Fig. 5. Performance of the affine control law (20) and the PWA control law (6)–(21) or (22) for the test grid from Fig. 4. The top row shows the two control laws as a function of the observation $\hat{\mathbf{y}}$, a transformed version of the measured voltage v_2 . The lower two rows show the resulting voltage magnitudes v_1 and v_2 . These should always remain between 0.95 pu and 1.05 pu. A linearized grid model is used to design the control laws in all cases, but for the experimental control evaluation here, we use both the linear model (LPF) and the underlying non-linear AC grid model (ACPF). The best affine control law for this example is not admissible, since the (unobserved) voltage magnitude v_1 is not guaranteed to be above 0.95 pu for realizations of the exogenous variables. In comparison, the computed general PWA control law keeps all voltage magnitudes valid under all circumstances.

from solving LPs (6)–(21) to evaluating (22). The proposed PWA control law is depicted in Fig. 5.

4) *Empirical ACPF Performance Assessment*: The obtained control laws, affine and PWA, are now applied to both the linearized power flow (LPF) and the ACPF equations to evaluate their performance in terms of state feasibility. To this end, a total of 625 realizations of (p_1, p_2) are generated on a 25×25 lattice that uniformly covers the set of exogenous actions \mathcal{D} . When applying the obtained control laws to the ACPF system, there may occur values of $\hat{\mathbf{y}}$ that do not belong to the set $\hat{\mathcal{Y}}$ —which is constructed based on the assumed linear representation of the power grid. For those values of $\hat{\mathbf{y}}$, we propose to choose the control action \mathbf{u} associated to the nearest point in $\hat{\mathcal{Y}}$.

The resulting voltages magnitudes v_1 and v_2 for both affine and PWA control laws are plotted in Fig. 5. Note that the lower operational limit for the unobserved voltage magnitude v_1 is violated for many high load situations when the affine control law (20) is applied to both the LPF and ACPF models. In contrast, the designed PWA control law keeps the voltage magnitudes feasible even for the ACPF system in this case. Further, the resulting range of voltage magnitudes is larger for the ACPF system compared to the LPF, particularly in high load situations (i.e., for low values of $\hat{\mathbf{y}}$ in Fig. 5).

In such situations, the line losses affect the validity of the lossless linearized Distflow equations significantly. This is because such linear power flow approximation in general underestimates the true line flows and overestimates the true voltage magnitudes across the distribution grid [18].

Also note in Fig. 5 that, as the value of q_2 is maximized, the voltage magnitudes obtained via the PWA control law are generally higher than the ones obtained for the affine control law. This is due to the added functional flexibility of the PWA approach as compared to the more restrictive affine setting.

Table I presents the obtained average solver times for computing the control action \mathbf{u} via the admissible PWA control law $\mathbf{u} = \mathbf{k}_{\text{opt}}(\hat{\mathbf{y}})$, for both online and offline approaches. While the online, one-stage approach is twice faster than its two-stage counterpart here, the explicit PWA control law outperforms both online approaches by 3 orders of magnitude.

TABLE I
SOLVER TIMES AVERAGED OVER 625 REALIZATIONS OF $\mathbf{d} \in \mathcal{D}$

Task for a given $\hat{\mathbf{y}}$	Solver time
Evaluate $\hat{\mathbf{z}}(\hat{\mathbf{y}})$ via first-stage LP (6)	1.9 ms
Compute optimal \mathbf{u} via second-stage LP (21)	1.8 ms
Compute optimal \mathbf{u} via one-stage LP derived from (10)	2.1 ms
Compute optimal \mathbf{u} via explicit PWA mapping (22)	4.8 μ s

B. Modified IEEE 123 Distribution Feeder

We now apply the proposed framework to a larger grid, namely a modified version of the IEEE 123 bus test case [27] as shown in Fig. 6. The power grid is assumed to be balanced, allowing us to perform single-line analysis. The system has a total of 86 PQ loads. The grid operator assumes that the i th load consumes active and reactive power in the ranges $[-p_i^{\text{peak}}, 0]$ pu and $[-q_i^{\text{peak}}, 0]$ pu, respectively. The peak load at each bus is calculated as the sum of the nodal spot load values specified in [27]. The system has a total peak load of $s_{\text{load}}^{\text{total}} = 14.36 + j7.84$ pu.

We add a total of 36 PV units as shown in Fig. 6. The active power injected by each PV unit is unknown to the grid operator but is limited by a maximum apparent power capacity of $s_{\text{PV}}^{\text{max}} = 0.344$ pu. While some PV units generate power with a power factor of 1, other PV units can inject reactive power to the grid, while being subject to the non-linear operational constraint $\sqrt{p_i^2 + q_i^2} \leq s_{\text{PV}}^{\text{max}}$. Similar to the use case studied in Section VI-A, each non-linear constraint is approximated with the help of 4 linear inequalities.

The goal of the grid operator is to keep all voltage magnitudes within the voltage band of 1 ± 0.05 pu. To this end, the grid operator communicates with the PV units at buses $\{74, 105\}$ to measure voltage magnitudes and adapt reactive power injections. Additionally, the grid operator can manipulate the voltage magnitude at buses $\{0, 8, 23, 71\}$ via on-load tap changers with ± 5 tap positions and a voltage resolution of 0.01 pu.

In line with the ideas of this paper and the above power grid specifications, we now define $\mathbf{u} = [q_{74} \ q_{105} \ v_0 \ v_8 \ v_{23} \ v_{71}]^T$, $\mathbf{y} = [v_{74} \ v_{105}]^T$, and the exogenous action $\mathbf{d} \in \mathcal{D} \subset \mathbb{R}^{244}$. Notice that a continuous control action space $\mathcal{U} \subset \mathbb{R}^6$ is assumed here. The matrices $\mathbf{G} \in \mathbb{R}^{254 \times 6}$, $\mathbf{H} \in \mathbb{R}^{254 \times 244}$, $\mathbf{N} \in \mathbb{R}^{2 \times 6}$, and $\mathbf{M} \in \mathbb{R}^{2 \times 244}$ are derived from the lossless, linearized DistFlow equations as in Example 1.

For this setting, the best affine control law $\mathbf{u} = \hat{\mathbf{K}}\hat{\mathbf{y}} + \hat{\mathbf{w}}$ is computed by solving the LP proposed in [8]. The LP is solved in ca. 1.68 s and yields $\eta_{\text{max}} = 0.0037 > 0$, i.e., an admissible affine control law does not exist. Subsequently, the existence of an admissible PWA control law is verified by solving QCQP (19). The solution of the proposed QCQP yields $\eta_{\text{max}} = -7.73 \times 10^{-4} \leq 0$, which confirms the existence of an admissible PWA control law. The QCQP is solved to global optimality in 16.65 s. Remarkably, an upper solution bound below 0 is obtained already after 3 s.

1) *Empirical ACPF Performance Assessment:* The performance of the online PWA control law implied by LPs (6)–(7) is now evaluated empirically when applied to the ACPF system.⁵ To this end, ACPF simulations are initially performed for three special situations, namely

- the Peak-Load-no-Generation (PLnG) situation,
- the Peak-Generation-no-Load (PGnL) situation, and
- the combined generation-consumption Worst-Case (WC) situation yielded by the optimal solution of QCQP (19).

⁵The closed-form representation of the PWA control law is not determined for this use case due to the enormous computational effort required to find the multiparametric solution of problem (11).

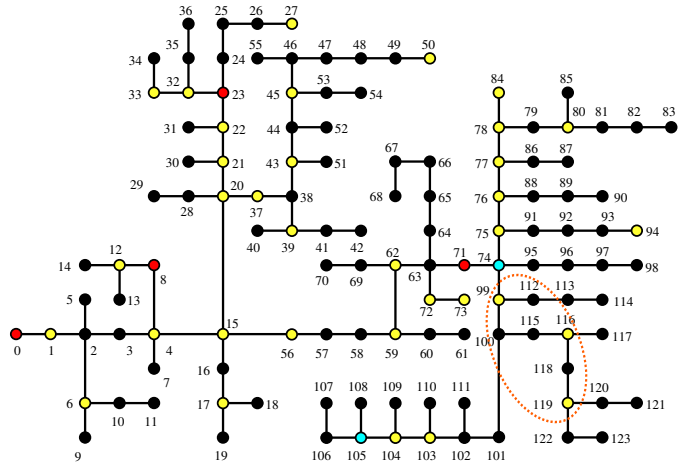


Fig. 6. Modified version of the IEEE 123 bus test case. The black circles correspond to load nodes and the substation transformer is located at node 0. The red circles indicate the location of voltage regulators. Those PV units that generate with power factor 1 are highlighted in yellow, and those having reactive power control and communication capabilities are colored in cyan. If the peak power capacity of all PV is increased by 5%, then possible overvoltages could be alleviated by additionally controlling the reactive power of the PV units connected to nodes $\{99, 116, 119\}$.

ACPF simulations are additionally executed for 2000 random realizations of the uncertain power injections sampled uniformly from the set \mathcal{D} .

When applying the PWA control law implied by LPs (6)–(7) to the ACPF system, there are two issues requiring special consideration. On the one hand, the mismatch between the LPF and ACPF models implies there could be observations for the ACPF system that lie outside the set $\hat{\mathcal{Y}}$ (which is constructed based on the assumed linear representation of the power grid). To overcome this, the authors propose to project such observations to the nearest point in $\hat{\mathcal{Y}}$. On the other hand, the controllable voltage magnitudes are manipulated via on-load tap changers here, which involves taking discrete control actions. We propose two variants for addressing the latter challenge. First, each voltage magnitude yielded by the PWA control law is rounded to the nearest point in the set of available voltage positions defined by $\mathcal{V} = \{0.95, 0.96, \dots, 1.04, 1.05\}$. This “LP+Round” variant is compared against the more complex control law that results when computing the discrete voltage magnitudes directly by solving the following Mixed-Integer Linear Program (MILP) online:

$$\begin{aligned} \mathbf{u} = \tilde{\mathbf{k}}(\hat{\mathbf{y}}) = & \arg \min_{\mathbf{u}' \in \mathbb{R}^{2 \times \mathcal{V}^4}} \min_{\eta \in \mathbb{R}} \eta \\ \text{s.t. } & \mathbf{G}\mathbf{u}' + \hat{\mathbf{z}}(\hat{\mathbf{y}}) \leq \mathbf{b} + \eta \mathbf{1}, \\ & -s_{\text{PV}}^{\text{max}} \leq u'_i \leq s_{\text{PV}}^{\text{max}}, \quad \forall i \in \{1, 2\}, \end{aligned} \quad (23)$$

where $\hat{\mathbf{z}}(\hat{\mathbf{y}})$ is defined by LP (6).⁶ In the following, MILP (23) is solved using a relative gap tolerance of 1×10^{-4} .

The results of the empirical ACPF study for both control variants are shown in Fig. 7. No voltage constraint violations

⁶It is assumed that the proposed “LP+Round” approach as well as the non-linear control law implied by LP (6) and MILP (23) are admissible in the sense of Definition 1. The derivation of an algorithm for verifying the existence of admissible control laws subject to mixed-integer control action spaces is left for future research.

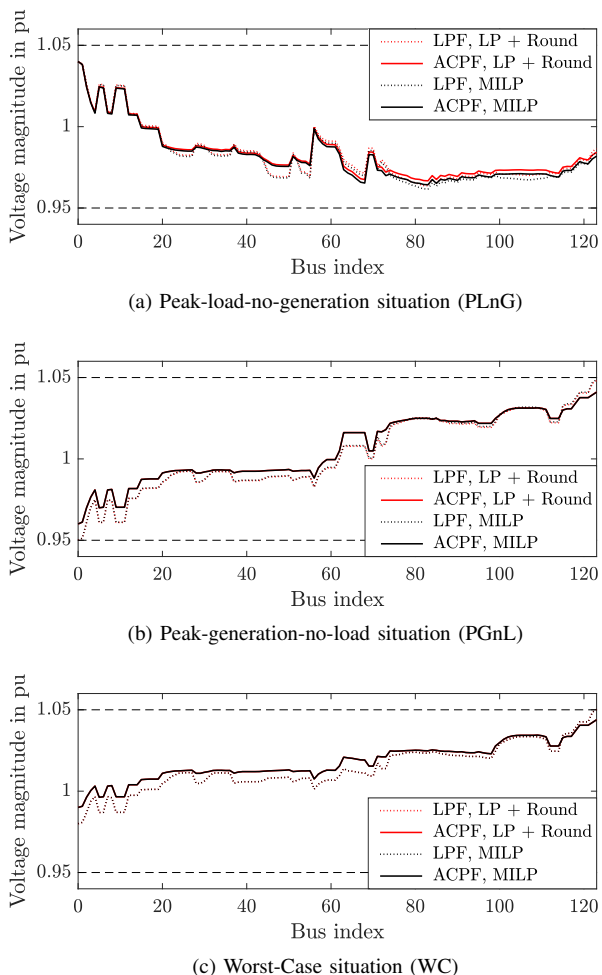


Fig. 7. Voltage magnitude profiles for the grid shown in Fig. 6. Three different critical situations are examined for different control variants and evaluation models. Remarkably, the most critical situation, i.e., with the voltage closest to the limits, is not obtained for the classically examined situations (Peak-Load-no-Generation and Peak-Generation-no-Load) but for a situation that combines power generation and consumption. It can be obtained via the proposed admissibility verification scheme (19).

occur over the 2003 tested realizations of the uncertain power injections. Moreover, the voltage profiles for the WC, PLnG, and PGnL situations are similar for the two compared control variants. While for the PLnG situation the voltage profiles differ slightly, for the WC and the PGnL situations the profiles are practically identical.

As indicated in Table II, the proposed online two-stage control variants have similar computational performance. In contrast, an alternative “LP+Round” variant based on the on-line one-stage LP (10) would almost double the computational effort due to the large number of auxiliary decision variables and constraints involved.

TABLE II
SOLVER TIMES AVERAGED OVER 2003 REALIZATIONS OF $d \in \mathcal{D}$

Task for a given \hat{y}	Solver time
Evaluate $\hat{z}(\hat{y})$ via first-stage LP (6)	0.66 s
Compute u via second-stage LP (7) + Round	2.14 ms
Compute u via second-stage MILP (23)	5.83 ms
Compute u via one-stage LP (10) + Round	1.25 s

2) *Effect of Increasing the Share of Solar PV:* We now increase the maximum capacity of all PV units by 5% and check whether an admissible PWA control law for this new setting exists. The optimal solution of QCQP (19) yields $\eta_{\max} = 4.37 \times 10^{-4} > 0$, meaning that the system does not admit any PWA control law. The QCQP is solved to global optimality in 4.76 s. The optimal value of $\alpha \in \mathbb{R}_{\leq 0}^{254}$ indicates that there is an overvoltage at bus 123. The overvoltage is caused by a joint peak PV generation, as can be read from the optimal value of d . This worst-case situation cannot be avoided by any control action. Additional controllable assets in the distribution grid are hence required.

We propose to additionally control the reactive power injected by the PV units at nodes $\{116, 119, 99\}$, as those PV units are the nearest to the bus presenting overvoltage. In the new setting, the optimal cost of QCQP (19) is $\eta_{\max} = -0.001 \leq 0$, corroborating the effectiveness of the proposed measure. The QCQP is solved to global optimality in ca. 5 min, and an upper bound below zero for the optimal value of η_{\max} is obtained already after 11 s. The proposed QCQP formulation is thus a powerful verification tool that can be implemented efficiently by using off-the-shelf optimization software. It allows grid operators to apply robust control algorithms with theoretical guarantees to safety-critical power flow control problems.

The proposed verification algorithm can also be exploited to find the minimum number of actuators and sensors required for the existence of an admissible PWA control law, e.g., by using hill climbing optimization as introduced previously in [8] for the case of affine control laws. In addition, the values of α and d obtained from the optimal solution of QCQP (19) provide valuable information about which operational constraints are critical and which realization of the exogenous actions leads (or may lead) to a (potential) constraint violation. This kind of analysis is paramount in current and future grid operation and grid planning activities over all grid voltage levels.

VII. CONCLUSION & OUTLOOK

This paper presents a novel model-based framework for the design of general admissible control laws for constrained linear power flow systems at steady state. Admissible control laws use imperfect system observations to determine suitable control actions that robustly guarantee a feasible power grid state independently of the influence of bounded exogenous actions. They additionally do not require a grid state estimation stage for computing the control action.

Supported by simulation experiments, this paper shows that there are realistic use cases in which affine control laws as proposed in [8] are not satisfying and more general control strategies are required. We establish that if there exists an admissible control policy for the constrained linear power flow system, then it can always be chosen as a piecewise-affine mapping with pieces defined on convex polytopes. Admissible PWA control laws can be computed online or offline depending on the specific problem instance as well as on the available software and hardware equipment. In particular, the online PWA control law implied by LPs (6)–(7) performs efficiently for the use cases considered in this paper.

The existence of admissible control laws for the constrained linear power flow system can be verified offline and with very reasonable computational efforts by solving QCQP (19). This enables the implementation of the proposed online PWA power flow controllers in safety-critical environments with theoretical guarantees already in the planning stage. Moreover, the offline verification step allows to design admissible PWA control laws that optimize techno-economic objectives. In case the power grid does not admit any PWA control law, the proposed QCQP also yields a realization of the exogenous action (e.g., uncertain power in-feeds) for which a feasible grid state cannot be guaranteed with the available actuators and sensors. This information is beneficial for grid operators in the planning stage, since it can support them when deciding if the installation of additional actuator and/or sensor devices is more adequate to alleviate grid contingency situations in comparison to traditional grid expansion measures.

Future work may apply the proposed approaches to other use cases that can be formulated using the abstract mathematical framework of constrained linear systems at steady state. Another line of research would be to make the explicit representation of the control law more compact, to avoid online optimization in the control loop. To this end, one could trade-off the number of pieces of the closed-form representation against a slightly larger feasibility indicator η , while still ensuring feasible grid states.

REFERENCES

- [1] J. Widén, E. Wäckelgård, J. Paatero, and P. Lund, “Impacts of distributed photovoltaics on network voltages: Stochastic simulations of three swedish low-voltage distribution grids,” *Electric Power Systems Research*, vol. 80, no. 12, pp. 1562–1571, 2010.
- [2] E. Veldman and R. A. Verzijlbergh, “Distribution grid impacts of smart electric vehicle charging from different perspectives,” *IEEE Transactions on Smart Grid*, vol. 6, no. 1, pp. 333–342, 2014.
- [3] A. Mešanović, U. Muenz, and C. Ebenbauer, “Robust optimal power flow for mixed ac/dc transmission systems with volatile renewables,” *IEEE Trans. on Pow. Sys.*, vol. 33, no. 5, pp. 5171–5182, 2018.
- [4] L. Roald and G. Andersson, “Chance-constrained ac optimal power flow: Reformulations and efficient algorithms,” *IEEE Transactions on Power Systems*, vol. 33, no. 3, pp. 2906–2918, 2017.
- [5] T. Mühlpfordt, L. Roald, V. Hagenmeyer, T. Faulwasser, and S. Misra, “Chance-constrained ac optimal power flow: A polynomial chaos approach,” *IEEE Trans. on Pow. Sys.*, vol. 34, no. 6, pp. 4806–4816, 2019.
- [6] S. Geng, M. Vrakopoulou, and I. A. Hiskens, “Chance-constrained optimal capacity design for a renewable-only islanded microgrid,” *Electric Power Systems Research*, vol. 189, p. 106564, 2020.
- [7] B. Pal and B. Chaudhuri, *Robust control in power systems*. Springer Science & Business Media, 2006.
- [8] E. Mora and F. Steinke, “On the minimal set of controllers and sensors for linear power flow,” *Elec. Pow. Sys. Res.*, vol. 190, p. 106647, 2021.
- [9] —, “Robust voltage regulation for active distribution networks with imperfect observability,” in *2021 IEEE Madrid PowerTech*, 2021.
- [10] D. K. Molzahn, F. Dörfler, H. Sandberg, S. H. Low, S. Chakrabarti, R. Baldick, and J. Lavaei, “A survey of distributed optimization and control algorithms for electric power systems,” *IEEE Transactions on Smart Grid*, vol. 8, no. 6, pp. 2941–2962, 2017.
- [11] T. Gal and J. Nedoma, “Multiparametric linear programming,” *Management Science*, vol. 18, no. 7, pp. 406–422, 1972.
- [12] E. N. Pistikopoulos, M. C. Georgiadis, and V. Dua, *Multi-Parametric Programming*. John Wiley & Sons, Ltd, 2007.
- [13] N. P. Faisca, V. Dua, and E. N. Pistikopoulos, *Multiparametric Linear and Quadratic Programming*. John Wiley & Sons, Ltd, 2007, pp. 1–23.
- [14] A. Bemporad, F. Borrelli, M. Morari *et al.*, “Model predictive control based on linear programming: the explicit solution,” *IEEE Transactions on Automatic Control*, vol. 47, no. 12, pp. 1974–1985, 2002.
- [15] A. Alessio and A. Bemporad, *A Survey on Explicit Model Predictive Control*. Berlin, Heidelberg: Springer, 2009, pp. 345–369.
- [16] M. N. Zeilinger, C. N. Jones, and M. Morari, “Real-time suboptimal model predictive control using a combination of explicit mpc and online optimization,” *IEEE Transactions on Automatic Control*, vol. 56, no. 7, pp. 1524–1534, 2011.
- [17] S. Boyd and L. Vandenberghe, *Convex Optimization*. USA: Cambridge University Press, 2004.
- [18] D. K. Molzahn and I. A. Hiskens, *A Survey of Relaxations and Approximations of the Power Flow Equations*. Now Foundations and Trends, 2019.
- [19] M. Baran and F. Wu, “Optimal capacitor placement on radial distribution systems,” *IEEE Transactions on Power Delivery*, vol. 4, no. 1, pp. 725–734, 1989.
- [20] —, “Optimal sizing of capacitors placed on a radial distribution system,” *IEEE Transactions on Power Delivery*, vol. 4, no. 1, pp. 735–743, 1989.
- [21] M. C. Ferris, O. L. Mangasarian, and S. J. Wright, *Linear programming with MATLAB*. SIAM, 2007.
- [22] G. Still, “Lectures on parametric optimization: An introduction,” *Optimization Online*, 2018.
- [23] M. Herceg, M. Kvasnica, C. Jones, and M. Morari, “Multi-Parametric Toolbox 3.0,” in *Proc. of the European Control Conference*, 2013, <http://control.ee.ethz.ch/~mpt>.
- [24] Gurobi Optimization, LLC, “Gurobi Optimizer Reference Manual,” 2021. [Online]. Available: <https://www.gurobi.com>
- [25] P. M. Castro, “Tightening piecewise McCormick relaxations for bilinear problems,” *Computers & Chemical Eng.*, vol. 72, pp. 300–311, 2015.
- [26] P. Kirst, O. Stein, and P. Steuermann, “An enhanced spatial branch-and-bound method in global optimization with nonconvex constraints [preprint],” *TOP*, 2015.
- [27] “IEEE 123 bus test case.” [Online]. Available: <https://site.ieee.org/pes-testfeeders/resources/>
- [28] J. Löfberg, “YALMIP: A toolbox for modeling and optimization in MATLAB,” in *Proc. of the CACSD Conference*, Taipei, Taiwan, 2004.
- [29] P. S. Kundur and O. P. Malik, *Power system stability and control*. McGraw-Hill Education, 2022.
- [30] R. D. Zimmerman and C. E. Murillo-Sanchez, “Matpower (version 7.1) [software],” 2020. [Online]. Available: <https://matpower.org>